Atmos. Chem. Phys., 16, 8081–8093, 2016
www.atmos-chem-phys.net/16/8081/2016/
doi:10.5194/acp-16-8081-2016

Atmospheric Chemistry and Physics Open Access EGU

Heterogeneous reactions of NO_2 with $CaCO_3$–$(NH_4)_2SO_4$ mixtures at different relative humidities

Fang Tan[1,2,*], Shengrui Tong[1,*], Bo Jing[1], Siqi Hou[1,2], Qifan Liu[1,2], Kun Li[1,2], Ying Zhang[1,2], and Maofa Ge[1,2]

[1]State Key Laboratory for Structural Chemistry of Unstable and Stable Species, Beijing National Laboratory for Molecular Sciences (BNLMS), Institute of Chemistry, Chinese Academy of Sciences, Beijing 100190, China
[2]University of Chinese Academy of Sciences, Beijing 100049, China
[*]These authors contributed equally to this work.

Correspondence to: Maofa Ge (gemaofa@iccas.ac.cn) and Shengrui Tong (tongsr@iccas.ac.cn)

Received: 27 January 2016 – Published in Atmos. Chem. Phys. Discuss.: 29 March 2016
Revised: 26 May 2016 – Accepted: 13 June 2016 – Published: 4 July 2016

Abstract. In this work, the heterogeneous reactions of NO_2 with $CaCO_3$–$(NH_4)_2SO_4$ mixtures with a series of weight percentage (wt %) of $(NH_4)_2SO_4$ were investigated using diffuse reflectance infrared Fourier transform spectroscopy (DRIFTS) at different relative humidity (RH) values. For comparison, the heterogeneous reactions of NO_2 with pure $CaCO_3$ particles and pure $(NH_4)_2SO_4$ particles, as well as the reaction of $CaCO_3$ with $(NH_4)_2SO_4$ particles, were also studied. The results indicated that NO_2 did not show any significant uptake on $(NH_4)_2SO_4$ particles, and it reacted with $CaCO_3$ particles to form calcium nitrate under both dry and wet conditions. The heterogeneous reactions of NO_2 with $CaCO_3$–$(NH_4)_2SO_4$ mixtures were markedly dependent on RH. Calcium nitrate was formed from the heterogeneous reactions at all the RHs investigated, whereas $CaSO_4 \cdot 0.5H_2O$ (bassanite), $CaSO_4 \cdot 2H_2O$ (gypsum), and $(NH_4)_2Ca(SO_4)_2 \cdot H_2O$ (koktaite) were produced depending on RH. Under the dry condition, the heterogeneous uptake of NO_2 on the mixtures was similar to that on $CaCO_3$ particles with neglectable effects from $(NH_4)_2SO_4$; the duration of initial stages and the NO_3^- mass concentrations had a negative linear relation with the mass fraction of $(NH_4)_2SO_4$ in the mixtures. Under wet conditions, the chemical interaction of $(NH_4)_2SO_4$ with $Ca(NO_3)_2$ enhances the nitrate formation, especially at medium RHs, while the coagulation of $(NH_4)_2SO_4$ with $CaCO_3$ exhibits an increasing inhibiting effects with increasing RH at the same time. In addition, the heterogeneous uptake of NO_2 on the mixtures of $CaCO_3$ and $(NH_4)_2SO_4$ was found to favor the formation of bassanite and gypsum due to the decomposition of $CaCO_3$ and the coagulation of Ca^{2+} and SO_4^{2-}. A possible reaction mechanism was proposed and the atmospheric implications were discussed.

1 Introduction

Haze with a high level of fine particulate matter with diameters less than 2.5 µm ($PM_{2.5}$) has occurred frequently in China in recent years (Fang et al., 2009; Kulmala, 2015). Emissions of gaseous pollutants, e.g., SO_2, NO_x, NH_3, and volatile organic compounds (VOCs), result in a series of atmospheric chemical reactions, which are responsible for the formation of secondary particles and the occurrence of haze (Zhang et al., 2015; Wang et al., 2013; Guo et al., 2014). Chemical analyses show that sulfate, nitrate, and ammonium are the major aerosol constituents of $PM_{2.5}$ (Yang et al., 2011; Huang et al., 2014). Pathak et al. (2009) discovered that nitrate concentration showed a correlation with sulfate concentration as well as the relative humidity (RH) value in ammonium-poor areas. Kong et al. (2014a) found strong negative correlation between the mass fraction of nitrate and that of sulfate in acidic atmospheric particles during air pollution episodes. Although atmospheric particulate sulfate, nitrate, and ammonium were found to be correlated by numerous field measurements in different locations (Sullivan et al., 2007; Quan et al., 2008; Duan et al., 2003; Possanzini et al., 1999; Querol et al., 1998), there is still a lack of knowledge to explain these phenomena.

Mineral dust is a major fraction of airborne particulate matter on a global scale (Tegen et al., 1996) with an estimated annual emission of 1000–3000 Tg of solids into the troposphere (Li et al., 1996). Mineral aerosols provide significant reactants and reactive sites for atmospheric heterogeneous reactions (Usher et al., 2003). Modeling studies indicated that mineral aerosols were highly associated with nitrate formation in the atmosphere (Dentener et al., 1996). Calcium carbonate represents an important and reactive mineral dust component, approximately accounting for 20–30 % of the total dust loading (Usher et al., 2003; Li et al., 2006; Al-Hosney and Grassian, 2005; Prince et al., 2007). Calcium carbonate particles are converted to calcium nitrate after reaction with nitrogen oxides and HNO_3 in the atmosphere (Li and Shao, 2009; Laskin et al., 2005). Field measurements reveal that mineral dust particles are often mixed with ammonium sulfate aerosols through coagulation during long-range transport (Levin et al., 1996; Zhang et al., 2000). Korhonen et al. (2003) suggested that ammonium sulfate coating of mineral dust by heterogeneous nucleation of H_2SO_4, NH_3, and H_2O could occur at atmospheric sulfuric acid concentration. Additionally, Mori et al. (1998) have found the coagulation between $CaCO_3$ and $(NH_4)_2SO_4$ could form koktaite and gypsum as a result of the interaction of ions under humid conditions. Ma et al. (2013) also discovered that mixed $CaCO_3$–$(NH_4)_2SO_4$ particles had synergistic effects on the formation of gypsum in the humidifying–dehumidifying processes.

A few studies have shown that coexisting components play a role in the heterogeneous uptake of trace gases on atmospheric particles. Kong et al. (2014b) found that coexisting nitrate could significantly accelerate the formation rate of sulfate on hematite surface, resulting in surface-adsorbed HNO_3, gas-phase N_2O and HONO productions. Zhao et al. (2013) found that coexisting surface nitrate had different effects on the uptake of H_2O_2 on mineral particle surfaces depending on RH. The catalytic and basic additives, e.g., MgO and $CaCO_3$, could increase the basic property of the surface of NaCl and increase the formation of sulfate by facilitating the absorbance of SO_2 on the alkaline surface (Li et al., 2007). To the best of our knowledge, the heterogeneous reaction of atmospheric trace gases on mixed $CaCO_3$–$(NH_4)_2SO_4$ particles has not been reported.

Furthermore, an increase in tropospheric NO_2 concentration has been observed in recent years across many developing regions due to fossil fuel combustion and biomass burning (Zhang et al., 2007; Sheel et al., 2010; Ghude et al., 2009; Shi et al., 2008; Richter et al., 2005; Irie et al., 2005). Atmospheric NO_2 concentration ranges from 70 parts per billion (ppb) during photochemical smog events to hundreds of parts per billion in polluted urban environments (Huang et al., 2015; Zamaraev et al., 1994). NO_2 is one such critical anthropogenic gaseous pollutant, which reduces air quality and affects global tropospheric chemistry. NO_2 plays a crucial role in the photochemical-induced catalytic production of ozone, leading to photochemical smog and increasing tropospheric ozone concentration (Volz and Kley, 1988). Moreover, the heterogeneous reactions of NO_2 can also lead to the deposition of nitric acid, as well as the formation of gas-phase HONO (Jaegle et al., 1998; Brimblecombe and Stedman, 1982; Goodman et al., 1999). Furthermore, the heterogeneous uptake of NO_2 on mineral aerosols was responsible for the nitrate accumulation in dust events (Usher et al., 2003). A number of laboratory studies investigated the heterogeneous reaction of NO_2 with mineral dust (Underwood et al., 1999b; Börensen et al., 2000; Finlayson-Pitts et al., 2003; Liu et al., 2015; Guan et al., 2014). Miller and Grassian (1998) discovered that NO_2 reacted with Al_2O_3 and TiO_2 particles to form surface nitrite and nitrate. Underwood et al. (1999a) measured the uptake coefficients of NO_2 on Al_2O_3, TiO_2, and Fe_2O_3 particles using a Knudsen cell. Li et al. (2010) determined the Brunauer–Emmett–Teller (BET) area-corrected initial uptake coefficients to be 10^{-9} and 10^{-8} for the heterogeneous uptake of NO_2 on $CaCO_3$ particles under dry and wet conditions, respectively. However, there are big gaps between the results of modeling studies and field measurements about the quantities and accumulation of nitrate, especially in haze periods (Zheng et al., 2015).

In the present study, the heterogeneous reactions of NO_2 with the mixtures of $CaCO_3$ and $(NH_4)_2SO_4$, pure $CaCO_3$ particles, and pure $(NH_4)_2SO_4$ particles at different RHs were investigated using a DRIFTS reactor. The surface adsorbed products were monitored and the uptake coefficients of NO_2 were determined. The aim of this work is to explore the kinetics and mechanism of the heterogeneous reactions of NO_2 with $CaCO_3$–$(NH_4)_2SO_4$ mixtures and its relevance to RH. The results are helpful for further exploring the correlations among particulate nitrate, sulfate, and ammonium concentration in the atmosphere and partly contribute to understanding of multicomponent reaction systems in practical environment conditions.

2 Experiment

$CaCO_3$ (99.5 %) and $(NH_4)_2SO_4$ (99.9 %) were purchased from Alfa Aesar. $CaCO_3$ and $(NH_4)_2SO_4$ were mechanically mixed and ground together in order to obtain uniform mixtures with 10–93 wt % (mass percent) of $(NH_4)_2SO_4$ in the mixtures, which were denoted as FAS-10, FAS-20, FAS-40, FAS-57, FAS-75, FAS-87, and FAS-93, respectively. The BET surface areas of pure $CaCO_3$ and $(NH_4)_2SO_4$ particles were determined to be 8.15 and 0.19 $m^2\,g^{-1}$, respectively, (Autosorb-1-MP automatic equipment (Quanta Chrome Instrument Co.)). The BET areas of the mixtures were determined to be 8.06, 6.62, 4.54, 3.21, 2.34, 1.67, and 0.89 $m^2\,g^{-1}$ corresponding to the mixtures mentioned above. NO_2 (0.1 %, Beijing Huayuan Gas Chemical Industry Co., Ltd.) and N_2 (> 99.999 %, Beijing Tailong Electronics Co., Ltd.) were used in this study.

In the gas supply system, N_2 was split into two streams; one was dehumidified by silica gel and molecular sieve to insure RH less than 1 %, which was called the dry condition; the other one was humidified by bubbling through ultrapure water. The flux of dry N_2, humid N_2, and NO_2 were adjusted to reach desired RH (< 1, 40, 60, and 85 % RH) conditions with the total flow of 400 sccm by using mass flow controllers (Beijing Sevenstar electronics Co., LTD). Concentration of NO_2 entering reactor was diluted to 2.6×10^{15} molecules cm^{-3} by mixing with N_2. RH and temperature of the inflow of sample cell were measured using a commercial humidity and temperature sensor (HMT330; Vaisala) with a measurement accuracy of ± 1 % RH and ± 0.2 °C, respectively.

In situ DRIFTS experiment was used to monitor reactions in real time without interrupting the reaction processes and provide mechanistic details and kinetic data (Vogt and Finlaysonpitts, 1994). Infrared spectra of sample surfaces were recorded with a Nicolet FTIR (Fourier transform infrared) Spectrometer 6700, which was equipped with a liquid-nitrogen-cooled narrowband mercury-cadmium-telluride (MCT) detector and DRIFTS optics (Model CHC-CHA-3, Harrick Scientific Corp.). The DRIFTS equipment has been described elsewhere (Tong et al., 2010). The spectra were measured at a resolution of 4 cm^{-1} in the spectral range from 4000 to 650 cm^{-1}. Each spectrum was generally averaged from 100 scans with a time resolution of 40 s. In situ DRIFTS experiments were carried out on $CaCO_3$–$(NH_4)_2SO_4$ mixtures, $CaCO_3$ particles, and $(NH_4)_2SO_4$ particles, respectively. Samples of about 30 mg were placed into the stainless steel sample holder (10 mm diameter, 0.5 mm depth). The investigated samples were exposed to pure nitrogen with desired RH for 20 min to establish adsorption equilibrium. Then infrared spectra of the unreacted powder samples were collected as background so that reaction products were observed as positive adsorption bands, while losses of surface species were observed as negative adsorption bands. Subsequently, NO_2 was introduced into the reaction chamber at a stable RH for 120 min. All the spectra were automatically collected through a Series program in OMNIC software.

The products formed on the samples after reaction with NO_2 were analyzed using ion chromatography (IC). The filtered solution was analyzed using a Dionex ICS 900 system, equipped with a Dionex AS 14A analytical column and a conductivity detector (DS5). The reacted samples were sonicated for 20 min in 8 mL ultrapure water.

3 Results and discussion

3.1 Surface products' characterization

Figure 1 represents the infrared (IR) spectra of surface products when the samples were exposed to NO_2 for 120 min at different RHs. Under the dry condition (Fig. 1a), absorption bands centered at 746, 816, 1040, 1300, and 1330 cm^{-1} which were assigned to surface nitrate could be observed on $CaCO_3$ particle surfaces (FAS-0) and the mixtures (Goodman et al., 2001, 2000; Al-Hosney and Grassian, 2005). Moreover, peaks at 1630 and 3540 cm^{-1} were assigned to crystal hydrate water in calcium nitrate (Li et al., 2010). It suggested that calcium nitrate was formed on $CaCO_3$ particle surfaces and the mixtures of $CaCO_3$ and $(NH_4)_2SO_4$. The detailed vibrational assignments were listed in Table 1. Two peaks observed at 1689 and 838 cm^{-1} could be attributed to the $\nu(C=O)$ and $\delta_{oop}(CO_3)$ of adsorbed carbonic acid, respectively, indicating that carbonic acid acted as an intermediate production under the dry condition (Al-Hosney and Grassian, 2004; Al-Abadleh et al., 2004). Besides, adsorbed nitric acid was also formed with peaks centered at 1710 and 1670 cm^{-1}, which were assigned to the asymmetric stretching of adsorbed nitric acid (Goodman et al., 1999). At the same time, negative bands ranging from 2800 to 3400 cm^{-1} could be ascribed to the loss of surface adsorbed water, and negative peaks at 3640 and 3690 cm^{-1} corresponded to the two types of hydroxyl ions on $CaCO_3$ particle surfaces (Kuriyavar et al., 2000). No obvious negative peaks could be observed when the samples were exposed to dry pure nitrogen for 120 min, which indicated that surface adsorbed water and hydroxyl ions participated in the reaction.

Compared with the spectrum of FAS-0, several additional weak absorptions appeared at 1008, 1096, and 1155 cm^{-1} on the $CaCO_3$–$(NH_4)_2SO_4$ mixtures, which could be attributed to the vibration modes of SO_4 tetrahedra in $CaSO_4 \cdot 0.5H_2O$ (bassanite) (Prasad et al., 2005; Liu et al., 2009). The vibration modes of water group in bassanite were too weak to be observed. In addition, the peak at 1215 cm^{-1} slightly grew in intensity during the whole heterogeneous reaction period of NO_2 with the mixtures, whereas it grew fast at the early stage of the reaction of NO_2 with $CaCO_3$ particles, and then diminished after reaching a maximum value at about 30 min (see Fig. S1 in the Supplement). This band described before was ascribed to nitrite species, which would convert to nitrate as the reaction proceeded (Miller and Grassian, 1998; Underwood et al., 1999b; Wu et al., 2013). To probe this product, samples after reaction with NO_2 for different times were detected by IC. The results showed that nitrite was increased during the first 30 min in the reaction of NO_2 with $CaCO_3$ particles, whereas there was too little to be detected after the reaction lasted about 60 min.

At 40 % RH (Fig. 1b), the absorption bands of nitrate shifted from 1040 to 1043 cm^{-1}, 746 to 749 cm^{-1}, and 816 to 828 cm^{-1}, respectively, compared to those under the dry condition. Meanwhile, the shoulder peak at 1300 cm^{-1} belong to asymmetric stretching of nitrate became ambiguous. The frequency shifts of nitrate adsorption bands were caused by the phase transition of calcium nitrate. It was reported that calcium nitrate was in an amorphous hydrated state at RH below 7 % (Liu et al., 2008), and it deliquesced to form a saturated solution droplet at 18 % RH (Tang and Fung, 1997). For the

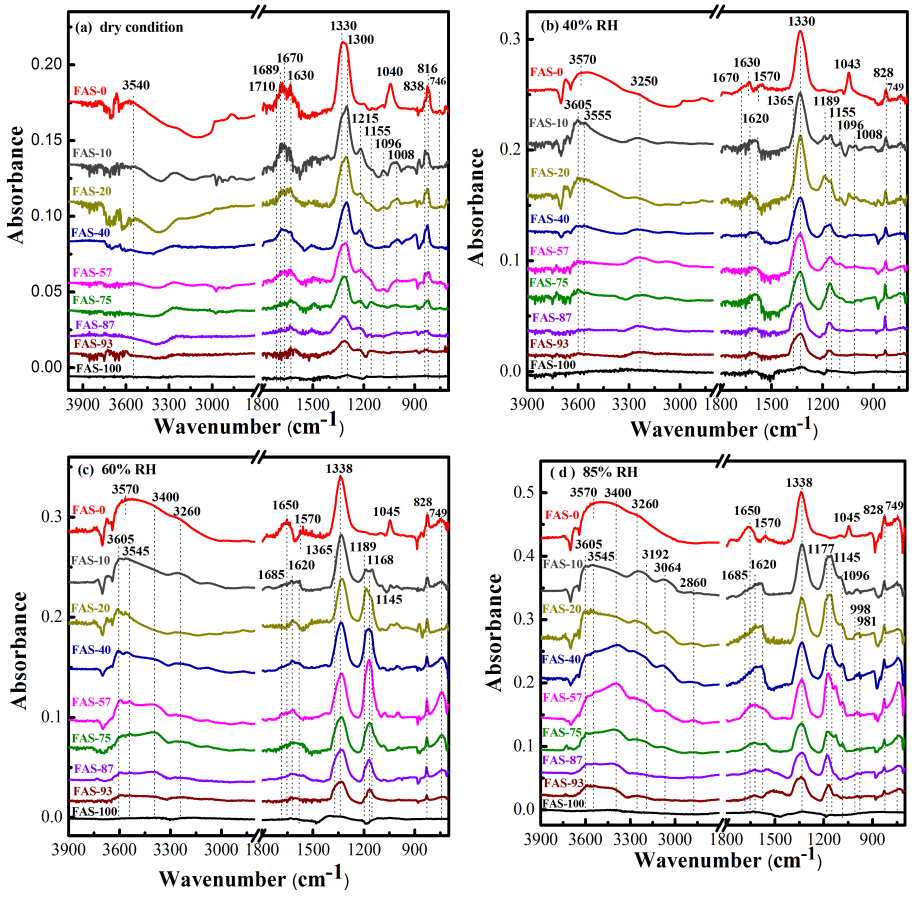

Figure 1. DRIFTS spectra of $CaCO_3$ particles (FAS-0), $CaCO_3$–$(NH_4)_2SO_4$ mixtures (FAS-10–FAS-93), and $(NH_4)_2SO_4$ particles (FAS-100) after reaction with NO_2 at **(a)** the dry condition, **(b)** 40 % RH, **(c)** 60 % RH, **(d)** 85 % RH for 120 min. The concentration of NO_2 was 2.6×10^{15} molecule cm^{-3}.

absorption bands of nitrate on the mixtures of $CaCO_3$ and $(NH_4)_2SO_4$, there was a new shoulder peak at 1365 cm^{-1} which were attributed to the $\nu_3(NO_3)$ in NH_4NO_3 (Schlenker et al., 2004). Moreover, the formation of $CaSO_4 \cdot 0.5H_2O$ was enhanced at 40 % RH compared to that under the dry condition, as features became apparent at 1155, 1096, and 1008 cm^{-1}, concomitant with the appearance of the peaks at 1620, 3555, and 3605 cm^{-1} due to the vibration modes of water group in bassanite (Prasad et al., 2005). Additionally, signatures at 1670 cm^{-1} and 1570 cm^{-1} on the samples suggested the formation of nitric acid and HCO_3^- during the heterogeneous reaction, respectively. In addition, the signature at 1189 cm^{-1} (Schlenker et al., 2004) on the mixtures suggested that HSO_4^- was produced.

When RH reached 60 % (Fig. 1c), water film was formed on particle surfaces with a band centered at 1650 cm^{-1} and a broad band composed of three peaks at 3260, 3400, and 3570 cm^{-1}, which could be assigned to the vibration modes of surface condensed water (Al-Abadleh et al., 2004). Meanwhile, the asymmetric stretching of surface nitrate appeared as a sharp peak at 1338 cm^{-1}. This was likely due to the fact that calcium nitrate incorporated into surface adsorbed water film and formed free aquated ions, based on the truth that only one sharp asymmetric stretching peak existed for free aquated ions NO_3^- (Gatehouse et al., 1957). The absorptions bands due to NH_4NO_3 could also be observed at 1365 cm^{-1} for the mixtures of $CaCO_3$ and $(NH_4)_2SO_4$. Additionally, new peaks could be observed at 1168, 1145, and 1117 cm^{-1}, which were attributed to the $\nu_3(SO_4)$ mode of gypsum. Although the IR absorption bands of bassanite and gypsum had some overlaps in the region between 1000 and 1250 cm^{-1}, there were some features that could be used to differentiate $CaSO_4 \cdot 0.5H_2O$ from $CaSO_4 \cdot 2H_2O$. Gypsum showed two IR-active modes in the bending modes of crystal hydrate water at 1620 and 1685 cm^{-1}, while bassanite had only one band at 1620 cm^{-1}. Additionally, the two stretching modes of crystal hydrate water appeared at 3545 and 3400 cm^{-1} for gypsum and at 3555 and 3610 cm^{-1} for bassanite (Prasad et al., 2005). Furthermore, it should be noticed that the peak at 3400 cm^{-1} from $CaSO_4 \cdot 2H_2O$ on the samples of FAS-40, FAS-57, FAS-75, and FAS-87 was much stronger than the peak at 3400 cm^{-1} from condensed

Table 1. Assignments of IR vibration frequencies of surface adsorbed species formed on $CaCO_3$ particle surfaces and $CaCO_3$–$(NH_4)_2SO_4$ mixtures.

Samples	Stretch mode	ν_1 (cm^{-1})	ν_2 (cm^{-1})	ν_3 (cm^{-1})	ν_4 (cm^{-1})	Stretch mode	
$Ca(NO_3)_2$	NO_3^-	1043	816	1300, 1330,	748		
[a]NH_4NO_3	NO_3^-	1050	830	1333, 1365		NH_4^+	1426, 1451
$CaSO_4 \cdot 0.5H_2O$	SO_4^{2-}	1008		1096, 1116, 1155, 1168		H_2O	1620, 3553, 3605
[b]$CaSO_4 \cdot 0.5H_2O$	SO_4^{2-}	1008		1096, 1116, 1153, 1168	601, 660	H_2O	1620, 3550, 3610
$CaSO_4 \cdot 2H_2O$	SO_4^{2-}	1003		1117, 1145, 1167		H_2O	1620, 1685, 3400, 3545
[c]$CaSO_4 \cdot 2H_2O$	SO_4^{2-}	1005		1117, 1145, 1167	602, 669	H_2O	1621, 1685, 3405, 3495, 3547
$(NH_4)_2Ca(SO_4)_2 \cdot H_2O$	SO_4^{2-}	981, 998		1131, 1177		H_2O	2860, 3064, 3192
[d]$(NH_4)_2Ca(SO_4)_2 \cdot H_2O$	SO_4^{2-}	981, 998		1108, 1131, 1177	602, 614, 646, 656	H_2O	2857, 2922, 3125, 3192

[a] from Schlenker et al. (2004). [b,c] from Prasad et al. (2005). [d] from Jentzsch et al. (2012).

water on $CaCO_3$ particles. Therefore it can be inferred that $Ca(NO_3)_2$, NH_4NO_3, $CaSO_4 \cdot nH_2O$ (gypsum and bassanite) were produced at 60 % RH from the heterogeneous reaction of NO_2 with the $CaCO_3$–$(NH_4)_2SO_4$ mixtures.

The spectrum of FAS-0 in Fig. 1d was similar to that in Fig. 1c, while there were considerable changes for spectra of the mixtures as RH increased to 85 %. Peaks observed at 981, 998, 1131, 1177 cm^{-1} on the mixtures due to the stretching vibration modes of SO_4^{2-} as well as peaks at 2860, 3064, 3192 cm^{-1} assigned to the stretching vibration modes of NH_4^+ indicated the formation of $(NH_4)_2Ca(SO_4)_2 \cdot H_2O$ (koktaite) (Jentzsch et al., 2012). The absorption band of nitrate overlapped with that of koktaite at 749 cm^{-1}. It can be inferred that koktaite, an intermediate production of gypsum, was formed rapidly as a result of the interaction of ions in the liquid film after the deliquescence of $(NH_4)_2SO_4$ and surface salts (Cziczo et al., 1997; Lightstone et al., 2000). Additionally, the IR absorption peaks at 1570 cm^{-1} in Fig. 1d are much stronger than those at 40 and 60 % RH. The positive intensity is likely due to the increasing information of HCO_3^-, which is from the decomposition of the bulk $CaCO_3$ under wet conditions. It can be interpreted that the reaction of NO_2 can occur not only on the surfaces of $CaCO_3$ and the mixtures but also into the bulk of the samples under wet conditions. Additionally, the acidity of surface condensed water is enhanced as a result of the formation of HNO_3 and the dissolution of $(NH_4)_2SO_4$, which facilitates the decomposition of bulk $CaCO_3$.

In conclusion, NO_2 did not show significant uptake on pure $(NH_4)_2SO_4$ particles (FAS-100) at all the RHs investigated. Additionally, the products formed from the heterogeneous reactions of NO_2 with $CaCO_3$–$(NH_4)_2SO_4$ mixtures were strongly dependent on RH. $Ca(NO_3)_2$ was produced under both dry and wet conditions; bassanite, gypsum, and koktaite were formed depending on RH.

In another set of experiments, the mixture of FAS-57 was exposed to nitrogen without the introduction of NO_2 in order to investigate the solid-state reaction of $CaCO_3$ with $(NH_4)_2SO_4$. As shown in Fig. 2, no new absorption bands occurred after exposing to dry nitrogen for 120 min. The weak peak at 1189 cm^{-1} due to HSO_4^- appeared as a main absorption peak and no obvious absorption band due to $CaSO_4 \cdot nH_2O$ could be observed at 40 % RH. The results suggested that little reaction occurred between $CaCO_3$ and $(NH_4)_2SO_4$ particles under the dry condition and 40 % RH. Therefore the chemical interaction of $Ca(NO_3)_2$ with $(NH_4)_2SO_4$ was responsible for the formation of bassanite in these conditions. This is likely due to the fact that $Ca(NO_3)_2$ is more hygroscopic and soluble than $CaCO_3$ particles. Furthermore, absorption bands attributed to bassanite, gypsum, koktaite, and surface water film could be observed at 60 and 85 % RH, indicating that a chemical reaction in the coagulation of $CaCO_3$ and $(NH_4)_2SO_4$ particles actually occurred without the introduction of NO_2 at 60 and

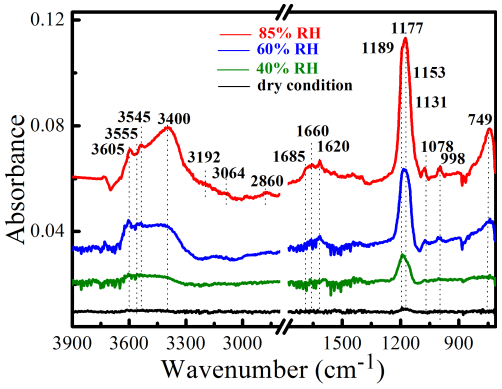

Figure 2. In situ DRIFTS spectra of surface products when the mixture of FAS-57 was exposed to nitrogen under the dry condition (black), 40 % RH (green), 60 % RH (blue) and 85 % RH (red) for 120 min.

85 % RH. This result was in good agreement with the results reported by Mori et al. (1998) that gypsum was formed from the chemical reaction between $(NH_4)_2SO_4$ and $CaCO_3$, with koktaite acting as an intermediate product at 70 % RH. In addition, the integrated absorbance of bands between 1100 and 1250 cm^{-1} for the sample of FAS-57 at 60 and 85 % RH in Fig. 2 were about 50 and 70 % of those for FAS-57 at corresponding RH in Fig. 1. Thus $CaSO_4 \cdot nH_2O$ and koktaite products could be formed both from the chemical interaction of $(NH_4)_2SO_4$ with $Ca(NO_3)_2$ and the reaction of $(NH_4)_2SO_4$ with $CaCO_3$ at 60 and 85 % RH.

3.2 Uptake coefficients and kinetics

The formation rates of nitrate on $CaCO_3$ particle surfaces and the mixtures were studied. The nitrate formed during the reaction was presented by the integrated absorbance (I_A) of the IR peak area between 1390 and 1250 cm^{-1}. The peak at 1043 cm^{-1} was not used to avoid the interruption of the absorptions of sulfates. The integrated nitrate absorbance over the ν_1 region (1013–1073 cm^{-1}) and the ν_3 region (1250–1390 cm^{-1}) could well overlap after the former multiplied by a constant on $CaCO_3$ particle surfaces (Fig. S2). Figure 3 represents the integrated absorbance of nitrate as a function of time at different RHs. The formation of nitrate on sample surfaces could be divided into three stages under the dry condition. The integrated absorbance of nitrate increased linearly with time in initial stage and it slowed down at stable stage after a transition period. Furthermore, the duration of initial stages for the mixtures decreased nearly linearly with increasing mass fraction of $(NH_4)_2SO_4$ in the mixtures; e.g., it lasted about 80 min for FAS-0 ($CaCO_3$ particles), 30 min for FAS-57, 20 min for FAS-75, and 5 min for FAS-93. In another word, the reactive ability of the mixtures in initial stage had a positive linear relation with the $CaCO_3$ content in the mixtures. The possible reasons were that for the reaction of NO_2 with $CaCO_3$–$(NH_4)_2SO_4$ mixtures, nitrate was formed by the uptake of NO_2 on $CaCO_3$ particle surfaces without the participation of $(NH_4)_2SO_4$ and the reactions limited on the particle surfaces under the dry condition. Moreover, the duration of initial stages was extended with increasing RH; e.g., it extended to 80 min for the mixture of FAS-75, to 50 min for the mixture of FAS-93, and even may be longer than 120 min for the mixtures with mass fraction of $(NH_4)_2SO_4$ smaller than 57 at 40 % RH. The boundaries between initial stages and transition stages became ambiguous at 60 % RH and finally disappeared at 85 % RH for all the $CaCO_3$–$(NH_4)_2SO_4$ mixtures. This was likely due to the fact that the reaction of NO_2 could react into the bulk of the particles under wet conditions.

The integrated absorbance (I_A) for nitrate ions on the samples had a linear relationship with the amount of nitrate determined by ion chromatography $\{NO_3^-\}$:

$$\{NO_3^-\} = I_A \times f. \quad (1)$$

Here f is the conversion factor. It is calculated to be $(2.14 \pm 0.17) \times 10^{17}$ ions/int.abs at 85 % RH and $(3.32 \pm 0.13) \times 10^{17}$ ions/int.abs at 60, 40 % RH, and the dry condition (see Fig. S3). The conversion factor f may change with the chemical environment of surface nitrate which is related to surface condensed water and ion interaction (Li et al., 2010). Then, nitrate formation rates $d\{NO_3^-\}/dt$ can be calculated from f and the slope of integrated absorbance as a function of time.

As shown in Fig. 4, the initial nitrate formation rates for the samples showed maximum values under the dry condition, whereas the stable formation rates were much slower in this condition. The initial nitrate formation rates increased slightly as RH increased from 40 to 60 and 85 % RH for the uptake of NO_2 on $CaCO_3$ particle surfaces (FAS-0). For the mixtures with mass fraction of $(NH_4)_2SO_4$ larger than 57 %, it showed an opposite variation that initial nitrate formation rates at 40 % RH were higher than that at 60 % RH, followed by that at 85 % RH. While for the mixtures with mass fraction of $(NH_4)_2SO_4$ smaller than 43 %, the nitrate formation rates increased initially as RH elevated from 40 to 60 % RH, then it decreased obviously as RH increased to 85 % RH. The differences in the tendency of nitrate formation rates with RH for the mixtures could be possibly explained by the combined opposite effects from the interaction of $(NH_4)_2SO_4$ with $Ca(NO_3)_2$ or $CaCO_3$ at 60 and 85 % RH.

Besides, nitrate formation rates decreased more evidently with increasing $(NH_4)_2SO_4$ content at 85 % RH and dry condition than at 40 and 60 % RH; e.g., the initial nitrate formation rates for the mixture of FAS-93 under the dry condition, 40, 60, and 85 % RH were 47, 70, 62, and 34 % of that for FAS-0 at corresponding RH, respectively. Furthermore as RH increased from the dry condition to 40 and 60 % RH, the initial nitrate formation rates decreased less for the reaction of NO_2 with the mixtures than with $CaCO_3$ particles, while it was opposite as RH increased to 85 % RH; e.g., the initial nitrate formation rates for FAS-0 at 40, 60, and 85 % RH

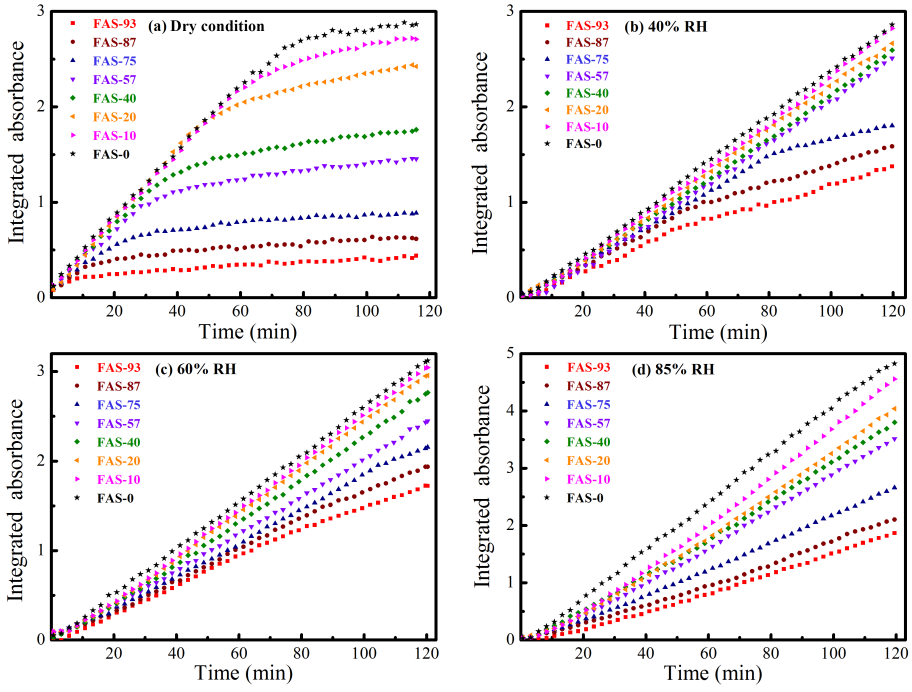

Figure 3. The integrated absorbance of the peak area between 1390 and 1250 cm^{-1} for nitrate on pure $CaCO_3$ particle surfaces (FAS-0), and $CaCO_3$–$(NH_4)_2SO_4$ mixtures (FAS-10–FAS-93) under **(a)** the dry condition, **(b)** 40 % RH, **(c)** 60 % RH, and **(d)** 85 % RH. The NO_2 concentration was 2.6×10^{15} molecule cm^{-3}.

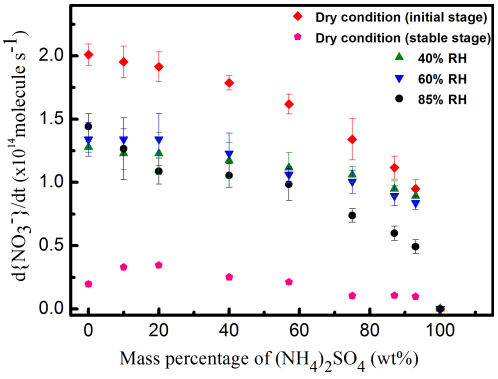

Figure 4. Initial nitrate formation rates at dry condition (rhombus), 40 % RH (triangle), 60 % RH (fall triangle), 85 % RH (roundness) and stable nitrate formation rates (pentagon) under the dry condition vs. the mass percentage of $(NH_4)_2SO_4$ in the mixtures. The data points and the error bars are the average value and the standard deviation of three duplicate experiments.

were 64, 67, and 72 % of those under the dry condition, respectively; for the mixture of FAS-93, the initial nitrate formation rates at 40, 60, and 85 % RH were 95, 87, and 60 % of those under the dry condition. In conclusion, the initial nitrate formation rates were accelerated to an extent at 40 and 60 % RH, whereas they were inhibited slightly at 85 % RH.

The reactive uptake coefficient (γ) is defined as the rate of the reactive collisions with the surface divided by the total number of surface collisions per unit time (Z):

$$\gamma = \frac{\mathrm{d}N(\mathrm{NO_2})/\mathrm{d}t}{Z} \tag{2}$$

$$Z = \frac{1}{4} A_{\mathrm{surface}} [\mathrm{NO_2}] \sqrt{\frac{8RT}{\pi M_{\mathrm{NO_2}}}}, \tag{3}$$

where $N(NO_2)$ is the number of reactive NO_2 collisions with the surface, $A_{surface}$ is the effective surface area of samples, and $[NO_2]$ is the gas-phase concentration of NO_2. R represents the gas constant, T represents the temperature, and M_{NO_2} is the molecular weight of NO_2. The rate of reactive NO_2 collision with the surface can be quantified in terms of the nitrate formation rate $\mathrm{d}\{NO_3^-\}/\mathrm{d}t$, then the reactive uptake coefficients can be calculated by

$$\gamma = \frac{\mathrm{d}\left\{\mathrm{NO_3^-}\right\}/\mathrm{d}t}{Z}. \tag{4}$$

The uptake coefficients of NO_2 on $CaCO_3$ particles and $CaCO_3$–$(NH_4)_2SO_4$ mixtures were calculated using both BET and geometric surface area, which could be considered as two extreme cases (Ullerstam et al., 2002). The results are listed in Table 2. The initial uptake coefficients corresponding to BET surface area for NO_2 on $CaCO_3$ particle surfaces are $(3.34 \pm 0.14) \times 10^{-9}$, $(2.04 \pm 0.07) \times 10^{-9}$, $(2.23 \pm 0.22) \times 10^{-9}$, and $(2.28 \pm 0.17) \times 10^{-9}$ for the dry condition, 40, 60, and 85 % RH, respectively, well consistent with previous measurement results (Li et al., 2010; Börensen

Table 2. Initial uptake coefficients calculated using BET surface area and geometric surface area for the reaction of NO_2 with $CaCO_3$ particle surfaces and $CaCO_3$–$(NH_4)_2SO_4$ mixtures at various RHs.

$(NH_4)_2SO_4$	Dry condition		40 % RH		60 % RH		85 % RH	
(wt %)	γBET ($\times 10^{-9}$)	γgeo ($\times 10^{-6}$)	γBET ($\times 10^{-9}$)	γgeo ($\times 10^{-6}$)	γBET ($\times 10^{-9}$)	γgeo ($\times 10^{-6}$)	γBET ($\times 10^{-9}$)	γgeo ($\times 10^{-6}$)
0	3.34 ± 0.14	10.4 ± 0.44	2.04 ± 0.07	6.36 ± 0.22	2.23 ± 0.22	6.94 ± 0.69	2.28 ± 0.17	7.10 ± 0.53
10	3.19 ± 0.21	9.83 ± 0.65	2.06 ± 0.21	6.34 ± 0.45	2.25 ± 0.14	6.91 ± 0.43	2.13 ± 0.41	6.56 ± 1.26
20	3.77 ± 0.24	9.54 ± 0.61	2.51 ± 0.34	6.28 ± 0.86	2.74 ± 0.42	6.87 ± 1.06	2.00 ± 0.21	5.63 ± 0.53
40	5.34 ± 0.17	9.25 ± 0.29	3.50 ± 0.42	6.07 ± 0.72	3.67 ± 0.48	6.36 ± 0.83	3.15 ± 0.28	5.46 ± 0.49
57	6.82 ± 0.33	8.38 ± 0.41	4.70 ± 0.51	5.78 ± 0.63	4.47 ± 0.26	5.49 ± 0.32	4.15 ± 0.53	5.10 ± 0.65
75	7.74 ± 0.94	6.94 ± 0.84	6.12 ± 0.37	5.49 ± 0.23	5.80 ± 0.53	5.20 ± 0.48	4.26 ± 0.31	3.82 ± 0.28
87	9.04 ± 0.73	5.78 ± 0.46	7.68 ± 0.50	4.92 ± 0.32	7.22 ± 0.63	4.63 ± 0.40	4.83 ± 0.46	3.10 ± 0.19
93	14.4 ± 1.07	4.90 ± 0.36	13.6 ± 0.93	4.63 ± 0.32	12.7 ± 0.81	4.34 ± 0.28	7.48 ± 0.82	2.55 ± 0.28

et al., 2000). The γ_{BET} is approximately a factor of 10^4 smaller than the $\gamma_{geometric}$. The γ_{BET} for the uptake of NO_2 on the mixtures was enhanced with increasing $(NH_4)_2SO_4$ content because of the decrease of BET surface area. On the contrary, the $\gamma_{geometric}$ decreased with increasing $(NH_4)_2SO_4$ content due to the decrease of nitrate formation rates.

The mass concentrations of NO_3^- formed on the samples after reaction with NO_2 were detected by IC, as shown in Fig. 5. The NO_3^- mass concentrations for $CaCO_3$ particles are 3.22 ± 0.17, 3.31 ± 0.03, 3.38 ± 0.35, and $3.47 \pm 0.32\,mg\,g^{-1}$ under the dry condition, 40, 60, and 85 % RH, respectively. It suggests that the NO_3^- mass concentration increases slightly with higher RH for the reaction of NO_2 with $CaCO_3$ particles. For the $CaCO_3$–$(NH_4)_2SO_4$ mixtures, the NO_3^- mass concentrations under the dry condition are obviously smaller than those at 85 % RH, and it exhibits maximum values at 40 or 60 % RH. In addition, it should be noticed that the NO_3^- mass concentrations nearly have a negative linear relation with $(NH_4)_2SO_4$ mass fraction in the mixtures under the dry condition. This result is in good agreement with the conclusions of Figs. 1a and 3 that the reaction of NO_2 with $CaCO_3$–$(NH_4)_2SO_4$ mixtures is very similar to the reaction of NO_2 with pure $CaCO_3$ particles under the dry condition and that $(NH_4)_2SO_4$ has little effect on the formation of NO_3^- in this condition. Moreover, the concentrations of NO_3^- of the mixtures under wet conditions are markedly larger than those under the dry condition. The NO_3^- mass concentrations increase much more for the mixtures than for pure $CaCO_3$ particles as RH elevated from the dry condition to wet conditions; e.g., the NO_3^- mass concentrations for the mixture of FAS-57 are 3.23 ± 0.09, 3.09 ± 0.14, and $2.42 \pm 0.07\,mg\,g^{-1}$ at 40, 60, and 85 % RH, respectively, which are increased by a factor of 2.1, 2.0, and 1.6 in comparison with that for FAS-57 under the dry condition ($1.55 \pm 0.08\,mg\,g^{-1}$). For the reaction of NO_2 with FAS-0, the NO_3^- mass concentrations just increase by a factor of 1.03, 1.05, and 1.08, as RH increased from the dry condition to 40, 60, and 85 % RH, respectively. These results clearly reveal that the $CaCO_3$–$(NH_4)_2SO_4$ mixtures exhibit promotive effects on nitrate formation in the heterogeneous reaction with NO_2 under wet conditions.

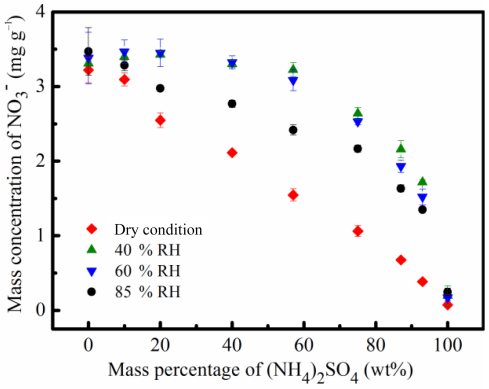

Figure 5. The mass concentration of NO_3^- for $CaCO_3$ particles and the $CaCO_3$–$(NH_4)_2SO_4$ mixtures after they reacted with NO_2 for 120 min as a function of the mass percentage of $(NH_4)_2SO_4$ in the mixtures. The data points and the error bars are the average value and the standard deviation of three duplicate experiments.

The results described above indicate that relative humidity plays a vital role in the heterogeneous reaction of NO_2 with $CaCO_3$–$(NH_4)_2SO_4$ mixtures. Under dry condition, little reaction occurs between $CaCO_3$ and $(NH_4)_2SO_4$. Therefore, nitrate formed on the mixtures under the dry condition is mainly produced from the reaction of NO_2 with $CaCO_3$ particles. At 40 % RH, the solid-state reaction between $CaCO_3$ and $(NH_4)_2SO_4$ particles can be neglected, implying that the solid-state reaction has little effect on the heterogeneous reaction. Meanwhile, the chemical interaction of $Ca(NO_3)_2$ with $(NH_4)_2SO_4$ is enhanced with the deliquescence of $Ca(NO_3)_2$, resulting in the formation of microcrystallites of NH_4NO_3 and $CaSO_4 \cdot nH_2O$. Consequently, it may help to improve the ionic mobility of the surface ions (Allen et al., 1996), modify the surface structure, and reexpose reactive sites (Al-Hosney and Grassian, 2005). Thus the chemical interaction of $Ca(NO_3)_2$ and $(NH_4)_2SO_4$ par-

ticles may exhibit promotive effects on the nitrate formation during the heterogeneous reaction of NO_2 with $CaCO_3$–$(NH_4)_2SO_4$ mixtures. The nitrate formation rates and nitrate concentrations increase slightly when RH increased from 40 to 60 % RH for the mixtures with mass percentage of $(NH_4)_2SO_4$ less than 43 %. However, it was opposite for the mixtures with mass percentage of $(NH_4)_2SO_4$ larger than 57 %. This could be possibly explained that there is a combined effect of the two opposing effects on nitrate formation from the interaction of $(NH_4)_2SO_4$ with $Ca(NO_3)_2$ or $CaCO_3$ during the heterogeneous reaction of the mixtures with NO_2. Since a chemical reaction in the coagulation of $CaCO_3$ with $(NH_4)_2SO_4$ actually occurred without the introduction of NO_2 at 60 % RH, leading to the formation of $CaSO_4 \cdot nH_2O$, $CaCO_3$ particles are partly consumed during the coagulation process and $CaSO_4 \cdot nH_2O$ formed in the coagulation may block reactive sites for further reaction. Thus, the solid state reaction between $CaCO_3$ and $(NH_4)_2SO_4$ particles exhibits inhibiting effects on the formation of nitrate on the mixtures. As for 85 % RH, the deliquescence of $(NH_4)_2SO_4$ and surface nitrate leads to more water uptake on the mixture surfaces. The inhibiting effects from the coagulation of $CaCO_3$ and $(NH_4)_2SO_4$ in water film become stronger at 85 % RH than at 60 % RH, resulting in the decrease of nitrate formation rates and nitrate concentrations at 85 % RH in comparison with those at 40 and 60 % RH.

3.3 Mechanism

According to the experimental observations described above, a reaction mechanism for the heterogeneous reactions of NO_2 with $CaCO_3$–$(NH_4)_2SO_4$ mixtures was proposed.

Gas-phase NO_2 attached to surface OH groups on $CaCO_3$ particle surfaces, as shown in Reaction (R1), where (g) is the gas phase and (ads) is the adsorbed phase.

$$\mathrm{S{-}OH + NO_2(g) \rightarrow S{-}OH\ldots NO_2(ads)} \quad \text{(R1)}$$

Börensen et al. (2000) proposed that two adsorbed-phase NO_2 molecules result in surface nitrate and nitrite products through a disproportionation reaction. Underwood et al. (1999b) suggested that NO_2(g) reacted to form adsorbed nitrite species initially and then react with another surface nitrite or with gas-phase NO_2 to form nitrate. Nitrite was detected by FTIR and IC in this study. The reaction process can be described as

$$\mathrm{2S{-}OH\ldots NO_2(ads) \rightarrow S\ldots NO_3^-(ads) + S\ldots NO_2^-(ads) + H_2O} \quad \text{(R2)}$$

$$\mathrm{2S\ldots NO_2^-(ads) \rightarrow S\ldots NO_3^-(ads) + NO(g)} \quad \text{(R3)}$$

$$\mathrm{S\ldots NO_2^-(ads) + NO_2(g) \rightarrow S\ldots NO_3^-(ads) + NO(g).} \quad \text{(R4)}$$

Under dry condition, the surface nitrate was in equilibrium with surface adsorbed water and adsorbed HNO_3 species (Reaction R5). Adsorbed H_2CO_3 can exist on $CaCO_3$ particle surfaces (Reaction R6) and there was weak chemical interaction between $Ca(NO_3)_2$ and $(NH_4)_2SO_4$ (Reaction R7).

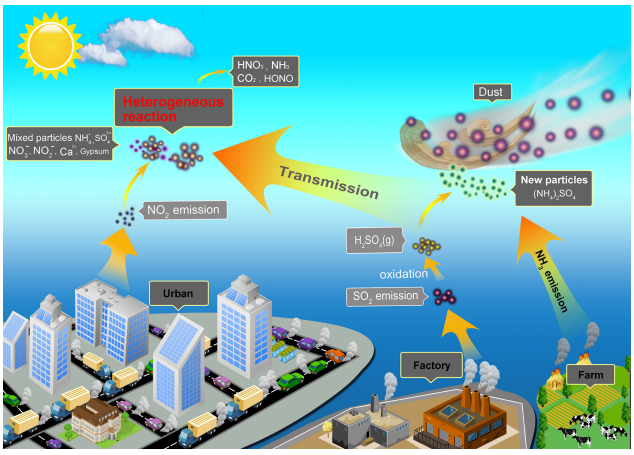

Figure 6. Schematic illustrating the possible heterogeneous processes of NO_2 with $CaCO_3$–$(NH_4)_2SO_4$ mixtures and the possible atmospheric implications.

$$\mathrm{S\ldots NO_3^-(ads) + S\ldots H_2O(ads) \rightarrow S\ldots HNO_3(ads) + S{-}OH} \quad \text{(R5)}$$

$$\mathrm{2S\ldots HNO_3(ads) + CaCO_3 \rightarrow Ca(NO_3)_2 + S\ldots H_2CO_3(ads)} \quad \text{(R6)}$$

$$\mathrm{Ca(NO_3)_2 \cdot nH_2O + (NH_4)_2SO_4 \rightarrow CaSO_4 \cdot nH_2O + 2NH_4NO_3} \quad \text{(R7)}$$

At 40 % RH, $Ca(NO_3)_2$ deliquesced to form a solution droplet and reacted with $(NH_4)_2SO_4$:

$$\mathrm{Ca^{2+} + 2NO_3^- + (NH_4)_2SO_4 + 0.5H_2O \rightarrow CaSO_4 \cdot 0.5H_2O + 2NH_4NO_3.} \quad \text{(R8)}$$

At 60 % RH, the interaction between $CaCO_3$ and $(NH_4)_2SO_4$ in the presence of surface adsorbed water film can be expressed as Reaction (R9):

$$\mathrm{2CaCO_3 + 3(NH_4)_2SO_4 \rightarrow (NH_4)_2Ca(SO_4)_2 \cdot H_2O + CaSO_4 \cdot nH_2O + 4NH_3 + 2CO_2.} \quad \text{(R9)}$$

It should be noticed that NH_3 was detected by PTR-MS (proton-transfer-reaction mass spectrometry) under wet conditions in this study. NH_3 can also be released from the decomposition of NH_4NO_3 (Reaction R10):

$$\mathrm{NH_4NO_3 \rightarrow NH_3 + HNO_3.} \quad \text{(R10)}$$

At the same time, the heterogeneous reaction of NO_2 with surface adsorbed water has been demonstrated to form adsorbed HNO_3(ads) and gaseous HONO(g) (Svensson et al.,

1987; Jenkin et al., 1988; Goodman et al., 1999):

$$H_2O(ads) + 2NO_2(ads) \rightarrow HNO_3(ads) + HONO(g). \quad (R11)$$

At 85 % RH, the interaction of ions in the water film can be expressed as

$$2Ca^{2+} + 3SO_4^{2-} + 2NH_4^+ + nH_2O \rightarrow CaSO_4 \cdot nH_2O + (NH_4)_2Ca(SO_4)_2 \cdot H_2O. \quad (R12)$$

4 Conclusions and atmospheric implications

The surface products and kinetics of the heterogeneous reactions of NO_2 with $CaCO_3$ particles, $(NH_4)_2SO_4$ particles, and $CaCO_3$–$(NH_4)_2SO_4$ mixtures were investigated under various RHs, using the DRIFTS technique. The solid-state reaction between $CaCO_3$ and $(NH_4)_2SO_4$ particles was also studied for comparison. All these reactions can occur in practical atmospheric conditions, which can be expressed in Fig. 6. The findings in this study have important atmospheric implications.

Calcium nitrate was produced from the heterogeneous reaction of NO_2 with $CaCO_3$–$(NH_4)_2SO_4$ mixtures under both dry and wet conditions, and bassanite, gypsum, and koktaite were formed depending on RH. It suggested that chemical composition in particulate phase was changed during the heterogeneous process, which can affect the physicochemical characteristics of atmospheric particles, including hygroscopicity, optical properties, and chemical reactivity. In addition, koktaite was detected in aerosols collected in Beijing, while it was absent in the soil where the dust originates (Mori et al., 2003); large uncertainties remain about its formation in the atmosphere. The results presented here provide evidence that the heterogeneous reactions of mixed $CaCO_3$–$(NH_4)_2SO_4$ particles with atmospheric acid trace gases were a possible source of koktaite. The results also indicated that the uptake of NO_2 and the formation of nitrate promoted removal of SO_4^{2-} from water-soluble species to insoluble gypsum species, which could reduce the atmospheric water soluble sulfate content.

Gas-phase products such as NH_3 could be released during the heterogeneous reaction of NO_2 with $CaCO_3$–$(NH_4)_2SO_4$ mixtures. In the atmosphere, NH_3 is mainly emitted from agriculture activities (such as fertilization and animal feeding) and biomass burning, and it plays an important role in nucleation and the growth of ion cluster and nanoparticles. The results in this study suggest that heterogeneous uptake of NO_2 on $CaCO_3$ particles with the presence of $(NH_4)_2SO_4$ may be a potential pathway for the transformation of NH_3 from particulate phase to gas phase.

Furthermore, the uptake coefficients of NO_2 on $CaCO_3$–$(NH_4)_2SO_4$ mixtures were determined, providing kinetic data for modeling studies. The results illustrate that the presence of $(NH_4)_2SO_4$ exhibits a promotive effect on the nitrate formation under wet conditions as a result of the interaction between $Ca(NO_3)_2$ and $(NH_4)_2SO_4$. On the contrary, the reaction between $CaCO_3$ and $(NH_4)_2SO_4$ particles has an inhibiting effect on the formation of nitrate during the heterogeneous reaction process, especially at high RH. Considering the abundance of $(NH_4)_2SO_4$ in the atmospheric aerosols, its mixtures with mineral dust may affect nitrate formation and the content of nitrate in atmospheric particles. The multicomponent reaction systems under ambient RH conditions play a potentially vital role in atmospheric processes. To better understand the role of heterogeneous reactions in the atmospheric chemistry, the effects of ambient RH (Rubasinghege and Grassian, 2013) as well as multicomponent reaction systems should be considered.

5 Data availability

All data are available upon request from the corresponding authors.

The Supplement related to this article is available online at doi:10.5194/acp-16-8081-2016-supplement.

Acknowledgements. This project was supported by the Strategic Priority Research Program (B) of the Chinese Academy of Sciences (grant no. XDB05010400), and the National Natural Science Foundation of China (contract no. 41475114, 91544227, 21477134).

Edited by: Y. Cheng

References

Al-Abadleh, H. A., Al-Hosney, H. A., and Grassian, V. H.: Oxide and carbonate surfaces as environmental interfaces: the importance of water in surface composition and surface reactivity, J. Mol. Catal. A-Chem., 228, 47–54, doi:10.1016/j.molcata.2004.09.059, 2004.

Al-Hosney, H. A. and Grassian, V. H.: Carbonic Acid: an important intermediate in the surface chemistry of calcium carbonate, J. Am. Chem. Soc., 126, 8068–8069, doi:10.1021/ja0490774, 2004.

Al-Hosney, H. A. and Grassian, V. H.: Water, sulfur dioxide and nitric acid adsorption on calcium carbonate: A transmission and ATR-FTIR study, Phys. Chem. Chem. Phys., 7, 1266–1276, doi:10.1039/b417872f, 2005.

Allen, H. C., Laux, J. M., Vogt, R., Finlayson-Pitts, B. J., and Hemminger, J. C.: Water-induced reorganization of ultrathin nitrate films on NaCl: Implications for the tropospheric chemistry of sea salt particles, J. Phys. Chem., 100, 6371–6375, doi:10.1021/jp953675a, 1996.

Börensen, C., Kirchner, U., Scheer, V., Vogt, R., and Zellner, R.: Mechanism and kinetics of the reactions of NO_2 or HNO_3 with alumina as a mineral dust model compound, J. Phys. Chem. A, 104, 5036–5045, doi:10.1021/jp994170d, 2000.

Brimblecombe, P. and Stedman, D. H.: Historical evidence for a dramatic increase in the nitrate component of acid-rain, Nature, 298, 460–462, doi:10.1038/298460a0, 1982.

Cziczo, D. J., Nowak, J. B., Hu, J. H., and Abbatt, J. P. D.: Infrared spectroscopy of model tropospheric aerosols as a function of relative humidity: Observation of deliquescence and crystallization, J. Geophys. Res.-Atmos., 102, 18843–18850, doi:10.1029/97jd01361, 1997.

Dentener, F. J., Carmichael, G. R., Zhang, Y., Lelieveld, J., and Crutzen, P. J.: Role of mineral aerosol as a reactive surface in the global troposphere, J. Geophys. Res.-Atmos., 101, 22869–22889, doi:10.1029/96jd01818, 1996.

Duan, F. K., Liu, X. D., He, K. B., Lu, Y. Q., and Wang, L.: Atmospheric aerosol concentration level and chemical characteristics of water-soluble ionic species in wintertime in Beijing, China, J. Environ. Monitor., 5, 569–573, doi:10.1039/b303691j, 2003.

Fang, M., Chan, C. K., and Yao, X.: Managing air quality in a rapidly developing nation: China, Atmos. Environ., 43, 79–86, doi:10.1016/j.atmosenv.2008.09.064, 2009.

Finlayson-Pitts, B. J., Wingen, L. M., Sumner, A. L., Syomin, D., and Ramazan, K. A.: The heterogeneous hydrolysis of NO_2 in laboratory systems and in outdoor and indoor atmospheres: An integrated mechanism, Phys. Chem. Chem. Phys., 5, 223–242, doi:10.1039/b208564j, 2003.

Gatehouse, B. M., Livingstone, S. E., and Nyholm, R. S.: Infrared spectra of some nitrato-co-ordination complexes, J. Chem. Soc., 847, 4222–4225, doi:10.1039/jr9570004222, 1957.

Ghude, S. D., Vander, R. J., Beig, G., Fadnavis, S., and Polade, S. D.: Satellite derived trends in NO_2 over the major global hotspot regions during the past decade and their inter-comparison, Environ. Pollut., 157, 1873–1878, doi:10.1016/j.envpol.2009.01.013, 2009.

Goodman, A. L., Underwood, G. M., and Grassian, V. H.: Heterogeneous reaction of NO_2: characterization of gas-phase and adsorbed products from the reaction, $2NO_2(g) + H_2O(a) \rightarrow HONO(g) + HNO_3(a)$ on hydrated silica particles, J. Phys. Chem., 103, 7217–7223, doi:10.1021/jp9910688, 1999.

Goodman, A. L., Underwood, G. M., and Grassian, V. H.: A laboratory study of the heterogeneous reaction of nitric acid on calcium carbonate particles, J. Geophys. Res., 105, 29053–29064, doi:10.1029/2000jd900396, 2000.

Goodman, A. L., Bernard, E. T., and Grassian, V. H.: Spectroscopic study of nitric acid and water adsorption on oxide particles: Enhanced nitric acid uptake kinetics in the presence of adsorbed water, J. Phys. Chem. A, 105, 6443–6457, doi:10.1021/jp003722l, 2001.

Guan, C., Li, X., Luo, Y., and Huang, Z.: Heterogeneous reaction of NO_2 on alpha-Al_2O_3 in the dark and simulated sunlight, J. Phys. Chem. A, 118, 6999–7006, doi:10.1021/jp503017k, 2014.

Guo, S., Hu, M., Zamora, M. L., Peng, J. F., Shang, D. J., Zheng, J., Du, Z. F., Wu, Z. J., Shao, M., Zeng, L. M., Molina, M. J., and Zhang, R. Y.: Elucidating severe urban haze formation in China, P. Natl. Acad. Sci. USA, 111, 17373–17378, doi:10.1073/pnas.1419604111, 2014.

Huang, K., Zhang, X., and Lin, Y.: The "APEC Blue" phenomenon: Regional emission control effects observed from space, Atmos. Res., 164, 65–75, doi:10.1016/j.atmosres.2015.04.018, 2015.

Huang, R. J., Zhang, Y., Bozzetti, C., Ho, K. F., Cao, J. J., Han, Y., Daellenbach, K. R., Slowik, J. G., Platt, S. M., Canonaco, F., Zotter, P., Wolf, R., Pieber, S. M., Bruns, E. A., Crippa, M., Ciarelli, G., Piazzalunga, A., Schwikowski, M., Abbaszade, G., Schnelle-Kreis, J., Zimmermann, R., An, Z., Szidat, S., Baltensperger, U., ElHaddad, I., and Prevot, A. S. H.: High secondary aerosol contribution to particulate pollution during haze events in China, Nature, 514, 218–222, doi:10.1038/nature13774, 2014.

Irie, H., Sudo, K., Akimoto, H., Richter, A., Burrows, J. P., Wagner, T., Wenig, M., Beirle, S., Kondo, Y., Sinyakov, V. P., and Goutail, F.: Evaluation of long-term tropospheric NO_2 data obtained by GOME over East Asia in 1996–2002, Geophys. Res. Lett., 32, L11810, doi:10.1029/2005gl022770, 2005.

Jaegle, L., Jacob, D. J., Brune, W. H., Tan, D., Faloona, I. C., Weinheimer, A. J., Ridley, B. A., Campos, T. L., and Sachse, G. W.: Sources of HO_x and production of ozone in the upper troposphere over the United States, Geophys. Res. Lett., 25, 1709–1712, doi:10.1029/98gl00041, 1998.

Jenkin, M. E., Cox, R. A., and Williams, D. J.: Laboratory studies of the kinetics of formation of nitrous-acid from the thermal-reaction of nitrogen-dioxide and water-vapor, Atmos. Environ., 22, 487–498, doi:10.1016/0004-6981(88)90194-1, 1988.

Jentzsch, P. V., Bolanz, R. M., Ciobota, V., Kampe, B., Roesch, P., Majzlan, J., and Popp, J.: Raman spectroscopic study of calcium mixed salts of atmospheric importance, Vib. Spectros., 61, 206–213, doi:10.1016/j.vibspec.2012.03.007, 2012.

Kong, L. D., Yang, Y., Zhang, S., Zhao, X., Du, H., Fu, H., Zhang, S., Cheng, T., Yang, X., Chen, J., Wu, D., Shen, J., Hong, S., and Jiao, L.: Observations of linear dependence between sulfate and nitrate in atmospheric particles, J. Geophys. Res.-Atmos., 119, 341–361, doi:10.1002/2013jd020222, 2014a.

Kong, L. D., Zhao, X., Sun, Z. Y., Yang, Y. W., Fu, H. B., Zhang, S. C., Cheng, T. T., Yang, X., Wang, L., and Chen, J. M.: The effects of nitrate on the heterogeneous uptake of sulfur dioxide on hematite, Atmos. Chem. Phys., 14, 9451–9467, doi:10.5194/acp-14-9451-2014, 2014b.

Korhonen, H., Napari, I., Timmreck, C., Vehkamaki, H., Pirjola, L., Lehtinen, K. E. J., Lauri, A., and Kulmala, M.: Heterogeneous nucleation as a potential sulphate-coating mechanism of atmospheric mineral dust particles and implications of coated dust on new particle formation, J. Geophys. Res.-Atmos., 108, 4546, doi:10.1029/2003jd003553, 2003.

Kulmala, M.: China's choking cocktail, Nature, 526, 497–499, 2015.

Kuriyavar, S. I., Vetrivel, R., Hegde, S. G., Ramaswamy, A. V., Chakrabarty, D., and Mahapatra, S.: Insights into the formation of hydroxyl ions in calcium carbonate: temperature dependent FTIR and molecular modelling studies, J. Mater. Chem., 10, 1835–1840, doi:10.1039/b001837f, 2000.

Laskin, A., Iedema, M. J., Ichkovich, A., Graber, E. R., Taraniuk, I., and Rudich, Y.: Direct observation of completely processed calcium carbonate dust particles, Faraday Discuss., 130, 453–468, doi:10.1039/b417366j, 2005.

Levin, Z., Ganor, E., and Gladstein, V.: The effects of desert particles coated with sulfate on rain formation in the eastern Mediter-

ranean, J. Appl. Meteorol., 35, 1511–1523, doi:10.1175/1520-0450(1996)035<1511:teodpc>2.0.co;2, 1996.

Li, H. J., Zhu, T., Zhao, D. F., Zhang, Z. F., and Chen, Z. M.: Kinetics and mechanisms of heterogeneous reaction of NO_2 on $CaCO_3$ surfaces under dry and wet conditions, Atmos. Chem. Phys., 10, 463–474, doi:10.5194/acp-10-463-2010, 2010.

Li, L., Chen, Z. M., Zhang, Y. H., Zhu, T., Li, J. L., and Ding, J.: Kinetics and mechanism of heterogeneous oxidation of sulfur dioxide by ozone on surface of calcium carbonate, Atmos. Chem. Phys., 6, 2453–2464, doi:10.5194/acp-6-2453-2006, 2006.

Li, L., Chen, Z. M., Zhang, Y. H., Zhu, T., Li, S., Li, H. J., Zhu, L. H., and Xu, B. Y.: Heterogeneous oxidation of sulfur dioxide by ozone on the surface of sodium chloride and its mixtures with other components, J. Geophys. Res.-Atmos., 112, D18301, doi:10.1029/2006jd008207, 2007.

Li, W. J. and Shao, L. Y.: Observation of nitrate coatings on atmospheric mineral dust particles, Atmos. Chem. Phys., 9, 1863–1871, doi:10.5194/acp-9-1863-2009, 2009.

Li, X., Maring, H., Savoie, D., Voss, K., and Prospero, J. M.: Dominance of mineral dust in aerosol light-scattering in the North Atlantic trade winds, Nature, 380, 416–419, doi:10.1038/380416a0, 1996.

Lightstone, J. M., Onasch, T. B., Imre, D., and Oatis, S.: Deliquescence, efflorescence, and water activity in ammonium nitrate and mixed ammonium nitrate/succinic acid microparticles, J. Phys. Chem. A, 104, 9337–9346, doi:10.1021/jp002137h, 2000.

Liu, Y., Wang, A., Freeman, J. J.: Raman, Mir, and NIR spectroscopic study of calcium sulfates: gypsum,bassanite, and anhydrite, 40th Lunar and Planetary Science Conference, 2009.

Liu, Y. J., Zhu, T., Zhao, D. F., and Zhang, Z. F.: Investigation of the hygroscopic properties of $Ca(NO_3)_2$ and internally mixed $Ca(NO_3)_2/CaCO_3$ particles by micro-Raman spectrometry, Atmos. Chem. Phys., 8, 7205–7215, doi:10.5194/acp-8-7205-2008, 2008.

Liu, Y. C., Han, C., Ma, J. Z., Bao, X. Z., and He, H.: Influence of relative humidity on heterogeneous kinetics of NO_2 on kaolin and hematite, Phys. Chem. Chem. Phys., 17, 19424–19431, doi:10.1039/c5cp02223a, 2015.

Ma, Q. X., He, H., Liu, Y. C., Liu, C., and Grassian, V. H.: Heterogeneous and multiphase formation pathways of gypsum in the atmosphere, Phys. Chem. Chem. Phys., 15, 19196–19204, doi:10.1039/c3cp53424c, 2013.

Miller, T. M. and Grassian, V. H.: Heterogeneous chemistry of NO_2 on mineral oxide particles: Spectroscopic evidence for oxide-coordinated and water-solvated surface nitrate, Geophys. Res. Lett., 25, 3835–3838, doi:10.1029/1998gl900011, 1998.

Mori, I., Nishikawa, M., and Iwasaka, Y.: Chemical reaction during the coagulation of ammonium sulphate and mineral particles in the atmosphere, Sci. Total Environ., 224, 87–91, doi:10.1016/s0048-9697(98)00323-4, 1998.

Mori, I., Nishikawa, M., Tanimura, T., and Quan, H.: Change in size distribution and chemical composition of kosa (Asian dust) aerosol during long-range transport, Atmos. Environ., 37, 4253–4263, doi:10.1016/s1352-2310(03)00535-1, 2003.

Pathak, R. K., Wu, W. S., and Wang, T.: Summertime $PM_{2.5}$ ionic species in four major cities of China: nitrate formation in an ammonia-deficient atmosphere, Atmos. Chem. Phys., 9, 1711–1722, doi:10.5194/acp-9-1711-2009, 2009.

Possanzini, M., De Santis, F., and Di Palo, V.: Measurements of nitric acid and ammonium salts in lower Bavaria, Atmos. Environ., 33, 3597–3602, doi:10.1016/s1352-2310(99)00096-5, 1999.

Prasad, P. S. R., Krishna Chaitanya, V., Shiva Prasad, K., and Narayana Rao, D.: Direct formation of the γ-$CaSO_4$ phase in dehydration process of gypsum: In situ FTIR study, Am. Mineral., 90, 672–678, doi:10.2138/am.2005.1742, 2005.

Prince, A. P., Grassian, V. H., Kleiber, P., and Young, M. A.: Heterogeneous conversion of calcite aerosol by nitric acid, Phys. Chem. Chem. Phys., 9, 622–634, doi:10.1039/b613913b, 2007.

Quan, J., Zhang, X., Zhang, Q., Guo, J., and Vogt, R. D.: Importance of sulfate emission to sulfur deposition at urban and rural sites in China, Atmos. Res., 89, 283–288, doi:10.1016/j.atmosres.2008.02.015, 2008.

Querol, X., Alastuey, A., Puicercus, J. A., Mantilla, E., Ruiz, C. R., Lopez-Soler, A., Plana, F., and Juan, R.: Seasonal evolution of suspended particles around a large coal-fired power station: Chemical characterization, Atmos. Environ., 32, 719–731, doi:10.1016/s1352-2310(97)00340-3, 1998.

Richter, A., Burrows, J. P., Nuss, H., Granier, C., and Niemeier, U.: Increase in tropospheric nitrogen dioxide over China observed from space, Nature, 437, 129–132, doi:10.1038/nature04092, 2005.

Rubasinghege, G. and Grassian, V. H.: Role(s) of adsorbed water in the surface chemistry of environmental interfaces, Chem. Rev., 49, 3071–3094, doi:10.1039/c3cc38872g, 2013.

Schlenker, J. C., Malinowski, A., Martin, S. T., Hung, H. M., and Rudich, Y.: Crystals formed at 293 K by aqueous sulfate-nitrate-ammonium-proton aerosol particles, J. Phys. Chem. A, 108, 9375–9383, doi:10.1021/jp047836z, 2004.

Sheel, V., Lal, S., Richter, A., and Burrows, J. P.: Comparison of satellite observed tropospheric NO_2 over India with model simulations, Atmos. Environ., 44, 3314–3321, doi:10.1016/j.atmosenv.2010.05.043, 2010.

Shi, C., Fernando, H. J. S., Wang, Z. F., An, X. Q., and Wu, Q. Z.: Tropospheric NO_2 columns over East Central China: Comparisons between SCIAMACHY measurements and nested CMAQ simulations, Atmos. Environ., 42, 7165–7173, doi:10.1016/j.atmosenv.2008.05.046, 2008.

Sullivan, R. C., Guazzotti, S. A., Sodeman, D. A., and Prather, K. A.: Direct observations of the atmospheric processing of Asian mineral dust, Atmos. Chem. Phys., 7, 1213–1236, doi:10.5194/acp-7-1213-2007, 2007.

Svensson, R., Ljungstrom, E., and Lindqvist, O.: Kinetics of the reaction between nitrogen-dioxide and water-vapor, Atmos. Environ., 21, 1529–1539, doi:10.1016/0004-6981(87)90315-5, 1987.

Tang, I. N. and Fung, K. H.: Hydration and Raman scattering studies of levitated microparticles: $Ba(NO_3)_2$, $Sr(NO_3)_2$, and $Ca(NO_3)_2$, J. Chem. Phys., 106, 1653–1660, doi:10.1063/1.473318, 1997.

Tegen, I., Lacis, A. A., and Fung, I.: The influence on climate forcing of mineral aerosols from disturbed soils, Nature, 380, 419–422, doi:10.1038/380419a0, 1996.

Tong, S. R., Wu, L. Y., Ge, M. F., Wang, W. G., and Pu, Z. F.: Heterogeneous chemistry of monocarboxylic acids on α-Al_2O_3 at different relative humidities, Atmos. Chem. Phys., 10, 7561–7574, doi:10.5194/acp-10-7561-2010, 2010.

Ullerstam, M., Vogt, R., Langer, S., and Ljungstrom, E.: The kinetics and mechanism of SO_2 oxidation by O_3 on

mineral dust, Phys. Chem. Chem. Phys., 4, 4694–4699, doi:10.1039/b203529b, 2002.

Underwood, G. M., Li, P., Usher, C. R., and Grassian, V. H.: Determining accurate kinetic parameters pf potentially important heterogeneous atmospheric reactions on solid particle surfaces with a Knudsen Cell Reactor, J. Phys. Chem. A, 104, 819–829, doi:10.1021/jp9930292, 1999a.

Underwood, G. M., Miller, T. M., and Grassian, V. H.: Transmission FT-IR and Knudsen Cell study of the heterogeneous reactivity of gaseous nitrogen dioxide on mineral oxide particles, J. Phys. Chem. A, 103, 6184–6190, doi:10.1021/jp991586i, 1999b.

Usher, C. R., Michel, A. E., and Grassian, V. H.: Reactions on mineral dust, Chem. Rev., 103, 4883–4939, doi:10.1021/cr020657y, 2003.

Vogt, R. and Finlaysonpitts, B. J.: A Diffuse Reflectance Infrared Fourier-Transform Spectroscopic (DRIFTS) study of the surface-reaction of NaCl with gaseous NO_2 and HNO_3, J. Phys. Chem., 98, 3747–3755, doi:10.1021/j100065a033, 1994.

Volz, A. and Kley, D.: Evaluation of the montsouris series of ozone measurements made in the 19th-century, Nature, 332, 240–242, doi:10.1038/332240a0, 1988.

Wang, Y., Zhang, Q. Q., He, K., Zhang, Q., and Chai, L.: Sulfate-nitrate-ammonium aerosols over China: response to 2000–2015 emission changes of sulfur dioxide, nitrogen oxides, and ammonia, Atmos. Chem. Phys., 13, 2635–2652, doi:10.5194/acp-13-2635-2013, 2013.

Wu, L. Y., Tong, S. R., and Ge, M. F.: Heterogeneous reaction of NO_2 on Al_2O_3: the effect of temperature on the nitrite and nitrate formation, J. Phys. Chem. A, 117, 4937–4944, doi:10.1021/jp402773c, 2013.

Yang, F., Tan, J., Zhao, Q., Du, Z., He, K., Ma, Y., Duan, F., Chen, G., and Zhao, Q.: Characteristics of $PM_{2.5}$ speciation in representative megacities and across China, Atmos. Chem. Phys., 11, 5207–5219, doi:10.5194/acp-11-5207-2011, 2011.

Zamaraev, K. I., Khramov, M. I., and Parmon, V. N.: Possible impact of heterogeneous photocatalysis on the global chemistry of the earths atmosphere, Cat. Rev.-Sci. Eng., 36, 617–644, doi:10.1080/01614949408013930, 1994.

Zhang, D. Z., Shi, G. Y., Iwasaka, Y., and Hu, M.: Mixture of sulfate and nitrate in coastal atmospheric aerosols: individual particle studies in Qingdao (36 degrees $04'$ N, 120 degrees $21'$ E), China, Atmos. Environ., 34, 2669–2679, doi:10.1016/s1352-2310(00)00078-9, 2000.

Zhang, Q., Streets, D. G., He, K., Wang, Y., Richter, A., Burrows, J. P., Uno, I., Jang, C. J., Chen, D., Yao, Z., and Lei, Y.: NO_x emission trends for China, 1995–2004: The view from the ground and the view from space, J. Geophys. Res.-Atmos., 112, D22306, doi:10.1029/2007jd008684, 2007.

Zhang, R. Y., Wang, G. H., Guo, S., Zamora, M. L., Ying, Q., Lin, Y., Wang, W. G., Hu, M., and Wang, Y.: Formation of urban fine particulate matter, Chem. Rev., 115, 3803–3855, doi:10.1021/acs.chemrev.5b00067, 2015.

Zhao, Y., Chen, Z. M., Shen, X. L., and Huang, D.: Heterogeneous reactions of gaseous hydrogen peroxide on pristine and acidic gas-processed calcium carbonate particles: Effects of relative humidity and surface coverage of coating, Atmos. Environ., 67, 63–72, doi:10.1016/j.atmosenv.2012.10.055, 2013.

Zheng, G. J., Duan, F. K., Su, H., Ma, Y. L., Cheng, Y., Zheng, B., Zhang, Q., Huang, T., Kimoto, T., Chang, D., Pöschl, U., Cheng, Y. F., and He, K. B.: Exploring the severe winter haze in Beijing: the impact of synoptic weather, regional transport and heterogeneous reactions, Atmos. Chem. Phys., 15, 2969–2983, doi:10.5194/acp-15-2969-2015, 2015.